

## NETLANDER SURFACE MODULE MOCKUP TESTING

T. Sproewitz<sup>1</sup>, J. Block<sup>2</sup>, R. Schuetze<sup>3</sup>, D. Arrat<sup>4</sup>, and A. Obst<sup>5</sup>

<sup>1</sup>Inst. of Comp. Structures & Adaptive Systems, DLR, 38108 Braunschweig, Germany, tom.sproewitz@dlr.de

<sup>2</sup>Inst. of Comp. Structures & Adaptive Systems, DLR, 38108 Braunschweig, Germany, joachim.block@dlr.de

<sup>3</sup>Inst. of Comp. Structures & Adaptive Systems, DLR, 38108 Braunschweig, Germany, rainer.schuetze@dlr.de

<sup>4</sup>Structural Department, CNES, 31401 Toulouse Cedex 4, France, denis.arrat@cnes.fr

<sup>5</sup>Mechanical Engineering Department, ESTEC, 2200 AG Noordwijk, The Netherlands, andreas.obst@esa.int

### ABSTRACT

In this paper it will be shown that at the DLR – Institute of Composite Structures and Adaptive Systems a Mars NetLander Surface Module mockup has successfully been designed and tested until the end of project Phase B. Focus is layed on experimental results that have already been gathered at this early stage and which will give confidence in the developed mathematical models and their assumptions.

In order to investigate the dynamical behavior of the Surface Module, resonance search tests were conducted and the compliance with the stiffness criterion could be proven.

Based on the mission two sizing load cases wrt. necessary structural strength were identified, which are part of the landing scenario in case of this lander mission. There are the first bounces onto Martian ground inside the airbag and the drop out-of-airbag onto Martian ground due to airbag ejection. Both load cases have experimentally been simulated at the premises of DLR.

For testing the drop inside the airbag a special test rig was designed which enabled to meet the required conditions very closely with a limited time and financial effort as low as possible. Desired output from these tests was to verify whether the drop-in-airbag would cause structural failures. Finally, the visual failure inspection did not reveal any failures for the Surface Module structure.

The drop out-of-airbag is considered to be the most stringent load case for the Surface Module design. Here, not only the structural strength, but also the structural responses to high shock loads are of great importance. A high number of tests was conducted with varying drop heights, Surface Module orientations and soil conditions. All tests conducted on a sandy ground did not cause any structural fail-

ures. The shock response spectra calculated from accelerometer data of all tests were examined and a shock response specification was derived. In this context it turned out that the shock loads due to the drop out-of-airbag do not exceed the shock loads induced by pyrotechnical events during the cruise phase.

By means of the conducted tests and their results it could be shown that a lander structure has been designed, which is capable of meeting the requirements necessary for a Mars Lander mission. Furthermore, the development of a very simple and cost effective test rig, which allows for cheap testing in early project phases, is presented.

Key words: NetLander, Testing, Shock Response, Drop Test, Sine Test.

## 1. INTRODUCTION

### 1.1. General Project Information



Figure 1. SurfM on Martian Ground

At the DLR – Institute of Composite Structures and Adaptive Systems the structure of the Mars NetLander SurfM (Surface Module) as part of the CNES – Mars Premier project was designed, built and tested until the end of Phase B (conf. Fig. 1).

The planned objective of the mission was to collect data by simultaneous measurements using a network of four identical landers spread over the Martian surface. Each lander should be equipped with scientific payload aimed at explorations of the interior of Mars, the atmosphere, the sub-surface, as well as of the ionospheric structure and geodesy. The launch was planned for 2009 and after a cruising phase of several months the Surface Modules should be separated from the orbiter and reach their landing sites. The necessary EDLS (Entry, Descent and Landing System) was based upon a heat shield, parachutes, and airbags. Therefore, other than for the majority of space missions, the sizing scenario for the structural design was not the launch, but the landing. Especially the first bounce onto Martian surface inside the airbags and the drop onto Martian ground after separation turned out to be the design driving load cases throughout the complete mission. The principle of the whole mission is depicted in Fig. 6.

A planetary lander capable of bearing extremely high acceleration up to  $180g$  and high shock loads due to a drop onto Martian ground from at least  $1m$  in compliance with the stiffness, thermal and mass requirements, which were predefined in this project, is only possible when fiber reinforced materials are used. Therefore all mechanically loaded structural parts except from mechanisms and low conductive heat links were mainly made from CFRP.

Already in the early project Phase B the development was based not only on FE analyses, but on mechanical test results as well. A mechanical mockup with realistic mass dummies was built and extensively tested as it will be lined out in the following paragraphs.

## 2. SURFACE MODULE STRUCTURE

The structural design of the SurfM is ruled by geometrical constraints, mainly from EDLS level, as well as by the expected mechanical and thermal loads. Resulting from the geometrical constraints of the already existing and successfully used EDLS system the SurfM main structure consists of:

- bowl shaped **Main Shell** which provides the three **EDLS Interface Brackets** (mechanical interfaces between SurfM and EDLS) and on which all payloads and subsystem devices are mounted (conf. Fig. 2)

- **Main Petal** which in stowed configuration serves as SurfM lid and in deployed configuration as solar array.
- **UM** (Uprighting Mechanism),  
**OM** (Opening Mechanisms),  
**FRM** (Fixation and Release Mechanisms)
- four **Secondary Petals** as carriers for solar arrays, which are stowed underneath the Main Petal and will be deployed by means of OM

Main Shell and Main Petal are made from CFRP (Carbon Fiber Reinforced Plastic) with a thickness of  $2mm$  and a quasi-isotropic lay-up. For reasons of mounting payloads and solar arrays, the double-curved parts of Main Shell and Main Petal are filled with aluminum honeycomb core, which is covered by a  $2mm$  thick CFRP plate providing a planar surface. At the free edge of the Main Petal a radial groove provides a form locking connection with the Main Shell. This leads to an increase of mechanical stiffness and prevents relative motions. Both structural parts are connected by the Main Hinge (Uprighting Mechanism). Furthermore the petal will be held down by a FRM on the Central Strut. The Central Strut is made from CFRP and lies in the rotational axis of the SurfM. The overall dimensions of the closed SurfM are  $580mm$  in diameter and  $290mm$  in height.

Figure 2 shows the Main Shell before integration in top view.

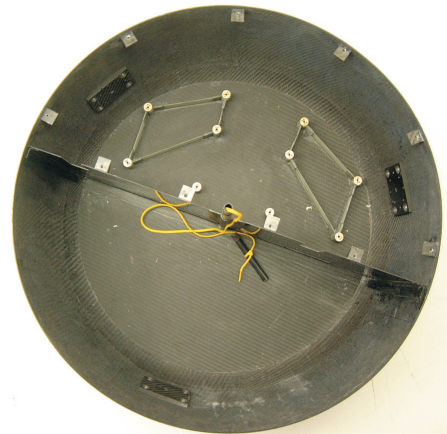


Figure 2. CFRP Main Shell with integrated SEC Interface Structure

As the SurfM performs scientific operations on the Martian surface it has to provide the above mentioned accommodation and mounting services. Furthermore it must ensure a proper thermal environment for the scientific instruments and system devices. For this reason the SurfM interior is divided into a payload bay and a thermally controlled SEC (SurfM Electronics Compartment) bay as can be seen in Figure 3. Furthermore there are shown all major structural parts and payload instruments.

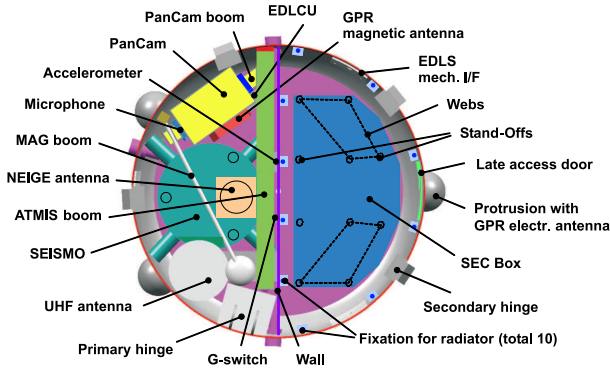


Figure 3. Scientific Payload and System Devices

In contrast to the payload bay, where the instruments can directly be fixed on the Mounting Plate, a low conductive support structure for the SEC box had to be designed. Reasons for this are the minimization of heat leaks and to provide an offset over the Mounting Plate, such that a 35 mm thick insulation material could be integrated. The SEC support structure is made from GFRP (Glass Fiber Reinforced Plastic) consisting of tubes and shear webs, which are glued into the honeycomb core between Main Shell and Mounting Plate. Depending on the load cases the tubes have to withstand high tensile, compression and bending loads. Therefore the lay-up is dominated by unidirectional fibres in tube longitudinal axis and sums up to 2 mm thickness. The webs, which mainly take shear forces, have a  $[\pm 45^\circ]$  lay-up and a thickness of 1 mm. In the top end of the GRFP tubes, aluminum inserts have been implemented to fix the SEC Base Plate on which all electrical devices are mounted. The SEC Base Plate is a 4 mm thick CFRP plate with a 0.1 mm copper layer for thermal control reasons.

The connection between tubes and inserts is designed such that pressure loads are transferred directly through the tube walls. For the case of high tensile loads the inserts have been sowed to the Main Shell using Kevlar rovings to ensure a low conductive link. For a better understanding how loads will be taken by the different structural parts and the different mechanisms like sowing in case of high tensile loads see Fig. 4.

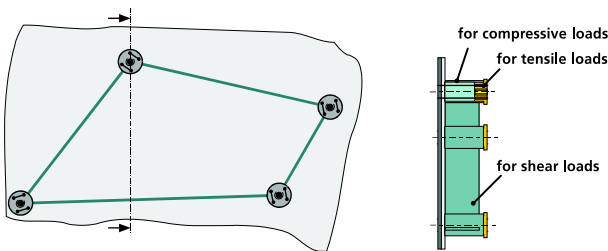


Figure 4. Principle of SEC Interface Structure

The mass of the NetLander SurfM as it is described herein adds up to 33.65 kg. A more detailed listing of the mass distribution is given in Table 1. In comparison to the total weight, the mass of the load bearing structural parts is less than 33% with 9665 g.

Table 1. SurfM Mass Budget

Structural / Payload Parts	Mass [g]
Platform	9665
Thermal Control System	3499
SEC	10170
Solar Arrays	1280
Payload	8202
Cabling (Payload)	837
<b>Total</b>	<b>33653</b>

Fig. 5 shows the coordinate axes definition by means of a Finite Element Model picture. The y-axis points along the "symmetry axis" of the SurfM. The z-axis is defined to lie in the separation plane between SEC and payload bay and the x-axis results directly according to the right hand rule.

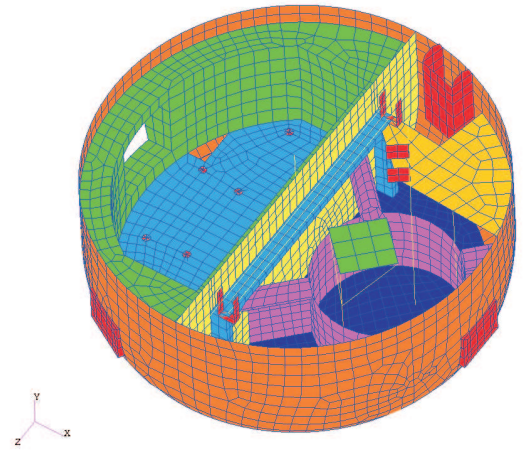


Figure 5. Coordinate System Definition

### 3. GENERAL LOAD CASE DEFINITION

In general the complete Earth-Mars transfer can be divided into three parts: launch, cruise and landing, where the landing can further be subdivided into entry, descent and landing on ground. All mechanically critical load cases for the above mentioned events were defined by the next higher level. Numbered according to the listing of flight phases in Fig. 6 the following main load cases were defined:

- 2 Quasistatic launch loads of  $\pm 45 g$  in one single axis combined with  $\pm 8 g$  in the lateral axes,
- 2,4,6 Stiffness requirement with a first global eigenfrequency of  $f_r \geq 150 Hz$ ,
- 2,6 Dynamical loads (sinusoidal, random) for launch and entry (heat shield supported aerodynamical breaking) phase,
- 6 Quasi-static entry loads (heat shield supported aerodynamical breaking) of  $\pm 36 g$  in a  $20^\circ$  cone around global y-axis,
- 7,8 Parachute deployment load of  $20 g$  during  $0.1 sec$  in a  $25^\circ$  cone,
- 13 First bounce onto Martian ground with  $180 g$  during  $0.2 sec$  in a  $45^\circ$  cone, Successive bounces with  $164 g$  in Surface Module lateral axes, Successive bounces upside down with  $121 g$  in a  $8^\circ$  cone and
- 14 Drop out-of-airbag with a drop height of  $1 m$ .

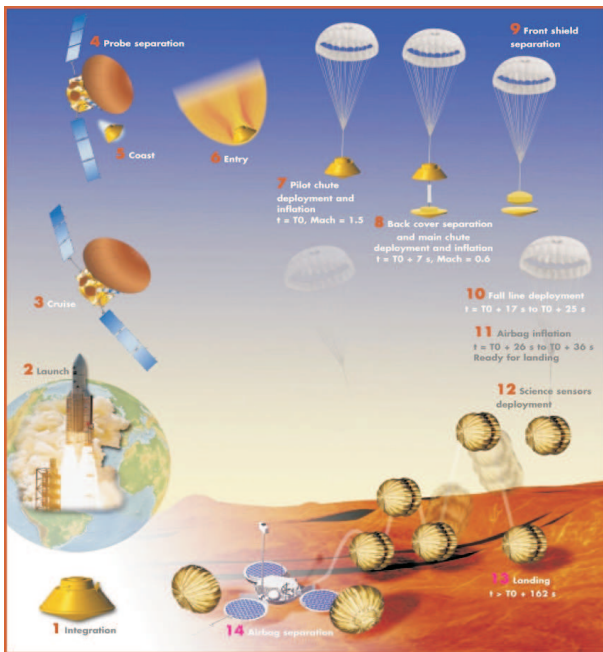


Figure 6. Surface Module Mission Scenario

Basically these load cases can be classified in stiffness and strength problems, though in some cases both might be of importance.

In terms of stiffness aspects focus was paid on the determination of the first global eigenfrequencies, regardless of mode shapes and modal effective masses. The results allow for a revision whether the structure meets the stiffness requirement with the current design. They allow also for a verification of

the accuracy of the numerical mathematical model in terms of dynamical problems. Hence, they are used to prove the quality of further analytical predictions. For this reason resonance search tests were conducted, which will be dealt with in Section 4.

Considering strength problems two severe load cases could be identified. There are the first bounces onto Martian surface inside the airbag (flight phase 13) and the drop out-of-airbag onto Martian ground (flight phase 14).

Throughout the investigations of the first load case structural failures are of major interest. Dynamical issues are not taken into account since the shock loads induce merely long duration half sine pulses compared to the required first global eigenfrequencies of the lander structure. Therefore these loads are considered to be quasi-static. A more comprehensive explanation of these tests will be given in Section 5.

The latter load case must, besides the strength problem, also be treated as dynamical problem, since the induced shock loads can be dangerous to the structure and the payload in particular, when the SurfM hits the Martian ground. This, of course, is strongly dependent on the predominant soil conditions, which can vary from loose sand, over scattered sharp-edged rocks, to hard flat rock. For both extremes tests were conducted as it is lined out in more detail in Section 6.

## 4. RESONANCE SEARCH TESTING

### 4.1. General Remarks and Requirements

The stiffness criterion for the Lander structure as issued by the next higher level, based on which the design was also driven, is as follows:

The SurfMSA shall have a first eigenfrequency with more than 10% of effective modal mass higher than  $150 Hz$ .

In order to prove the performance of the structure for the above mentioned requirement, resonance search tests as low level sine sweep with single axis base excitation were accomplished. These tests aimed at the identification of eigenfrequencies in a range of  $0 Hz \leq f \leq 2000 Hz$ . Main interest, however, was paid to the lowest global eigenfrequencies. Another point of great interest in this context was to verify the accomplished Finite Element model. Although a correlation would not be possible with the gained results, a comparison would give confidence in the modeling principle and assumptions.

All tests were carried out at the premises of the DLR

Institute of Composite Structures and Adaptive Systems, Section: System Conditioning in Berlin.

#### 4.2. Test Setup and Specifications

Two resonance search test runs were conducted using a TIRAVIB 51010/LS shaker with the appropriate measurement devices. Technical specifications for the shaker and data acquisition are given in the listings hereafter. Fig. 7 shows the test set-up with the Solar Arrays still in deployed configuration for reasons of accelerometer application in the interior. Throughout the tests the Solar Arrays will be in stowed configuration resembling the real conditions under which the SurfM will dynamically be loaded. In the set-up shown, the SurfM is already mounted on the shaker table by means of an aluminum adapter.

This adapter is a reinforced handling device for the SurfM. Although it is not ideally stiff it is considered to be adequate for the low level resonance search tests on breadboard level in such an early phase. A test prediction was conducted by means of FE analyses. In combined configuration (SurfM - mounting device) a drop of max. 2% in the first global eigenfrequencies up to 300 Hz was computed.



Figure 7. Opened Surface Module mounted on Sine Vibration Generator

**Shaker:** TRAVIB 51010/LS with slip table (TIRA Maschinenbau GmbH Rauhenstein, Germany)

max. force in sine mode:	11000 N
max. force in random mode:	11000 N
max. displacement peak to peak:	51 mm
max. velocity:	1.8 m/sec
max. acceleration;	950 m/sec <sup>2</sup>
frequency range:	2 – 5000 Hz

#### Acceleration Measurement:

- Charge Amplifier:

- 7 one-channel charge amplifier SWE 366 (RMS Regelungs- und Messtechnik Dynamic Test Systems Reinbeck, Germany)
- 4 four-channel charge amplifier NEXUS (Brüel & Kjær Nærum, Denmark)

- Single-Axis Transducer: (Brüel & Kjær Nærum, Denmark)
  - Accelerometer Type 4371 is a DeltaShear<sup>®</sup>, UniGain<sup>®</sup> type with side connector
  - Accelerometer Type 4375/4375V is a miniature DeltaShear<sup>®</sup> charge accelerometer
- Control unit VibControl NT m+p international (m+p international Mess- und Rechentchnik GmbH Hannover, Germany)

For the identification of the eigenfrequencies 6 accelerometers were used. Their location was chosen based on test prediction analyses and accessibility. Two pilot accelerometers were mounted on the shaker table for control reasons.

Due to the mounting of the SurfM in the helling it could not be tested directly in the lateral x- and z-axis. Moreover the two axes are rotated 30° about y-axis leading to:

- 1<sup>st</sup>-axis: 30° from z-axis about y-axis
- 2<sup>nd</sup>-axis: 30° from x-axis about y-axis

For both tests the following specifications were defined:

frequency range	5 – 2000 Hz
excitation acceleration	0.5 g
sweep rate	2 oct/min (one up-sweep)

In the tests an upward sweep was considered only. Due to the chosen sweep rate a distortion of the frequency response function should not appear as it is lined out by Ewins (1995).

#### 4.3. Resonance Search Test Results

In Table 2 there are listed the identified first eigenfrequencies for the two axes and all accelerometers. They are ordered according to the value of the eigenfrequencies. It can be seen that all global eigenfrequencies are above the 150 Hz requirement.

Figure 8 shows the recorded data of the accelerometer mounted on the Main Shell of the SEC bay. Slight amplifications can also be seen at about 130 Hz. These frequencies comply very well with the predicted data from FE analyses were the following values were analyzed:

Table 2. Resonance Survey Results

Axis	Accelerometer	Eigenfrequency
1 <sup>st</sup> -Axis	MP 4	182.3 Hz
	MP 3	187.7 Hz
	MP 1	203.7 Hz
	MP 5	203.7 Hz
	MP 6	203.7 Hz
	MP 2	206.1 Hz
2 <sup>nd</sup> -Axis	MP 4	180.1 Hz
	MP 1	196.7 Hz
	MP 3	197.8 Hz
	MP 6	200.2 Hz
	MP 2	207.3 Hz
	MP 5	216.0 Hz

$$f_1 = 135 \text{ Hz} \quad f_2 = 182 \text{ Hz}$$

$$f_3 = 200 \text{ Hz} \quad f_4 = 203 \text{ Hz}$$

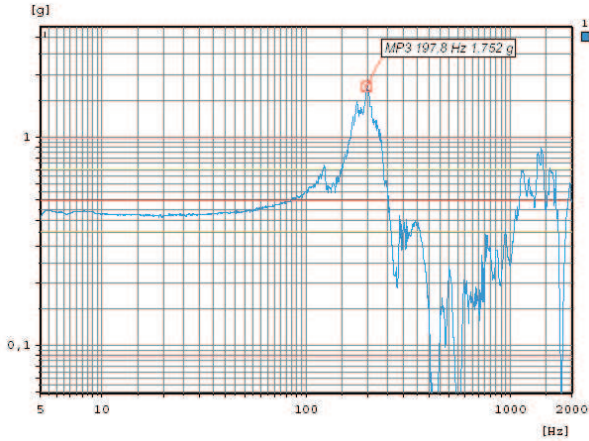


Figure 8. Frequency Response Function of MP 3 for 2<sup>nd</sup>-axis

The resonance search tests conducted on the SurfM breadboard model showed that the designed structure fulfills the above mentioned stiffness criterion.

## 5. DROP IN-AIRBAG TESTING

### 5.1. General Remarks and Requirements

As already pointed out in Section 3 the first bounces on the martian ground inside the airbags are one of the design driving scenarios throughout the complete mission. Especially the first bounce with a well defined load vector and the second bounce which can

have arbitrary orientations are of particular interest. The severity of these load cases led to the request for tests under realistic conditions before the PDR (Preliminary Design Review) in order of being able to incorporate necessary changes in the structural design. For completeness the requirement for the first bounce as defined by the next higher level is reiterated hereafter:

The SurfMSA, rounded by cloth of the airbag, shall withstand the loads defined as the cumulative effect of:

- a pressure of 37 kPa all around the station
- a field of acceleration of 180 g, half sine 20 ms in a cone of  $\pm 45^\circ$  angle around  $Y_s$ -axis

The specific aim of the conducted tests are as follows:

- verification whether the SurfM structure can withstand the high loads without getting damaged to an extent that endangers the mission
- gain knowing about the structural behavior.

Fig. 9 shows the SurfM embedded in the airbag. The fixation of the SurfM inside the two airbag halves is realized by means of belts (conf. Fig. 11), which surround the SurfM, and by means of ropes, which connect the airbag to these belts. When bouncing onto Martian ground all loads will be taken by the belts and by the skirt of the inflated airbag, which completely envelops the SurfM.

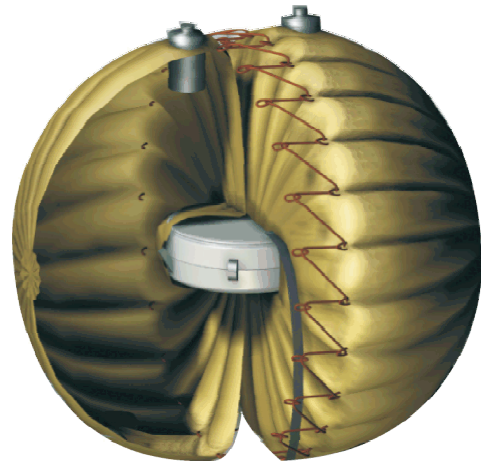


Figure 9. Surface Module wrapped in Airbag

Three specific worst cases were identified. Fig. 10 shows the principle of the derivation of the landing loads inside the airbag. In Table 3 there are listed the loads that may have to be expected. They already include a margin leading to qualification level. These loads were originally provided by the airbag

manufacturer. Given are the belt forces and the total forces acting on the SurfM. The difference from both leads directly to the load that will be induced by the airbag skirt. No belt forces are provided in the third case, since the load vector will be in lateral z-direction, which is perpendicular to the belts. Hence, the belts do not take any loads.

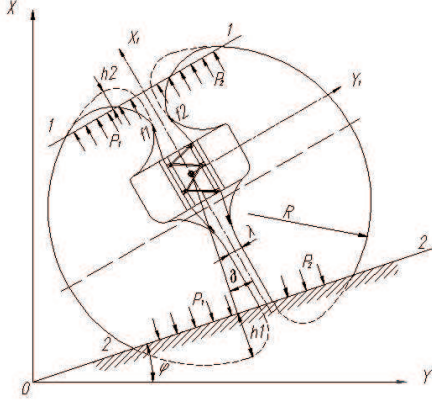


Figure 10. Principle of in Airbag Load Case (Courtesy of Babakin Space Center)

A structural mass of 36 kg is assumed to evaluate the apparent g-loads. However, for the first bounce an even higher load of 180 g was defined. The deceleration profile shall be a half sine pulse with a duration of 20 msec.

Table 3. Drop In-Airbag Loads Definition

Load Case Bounces	Belt Forces [N]	Total Forces [N]	G-Load [g]
First	40420	55220	156
Second upside down	34640	42745	121
Second lateral	—	42745	164

For these tests focus was put on generating such high g-loads with the specified profile. To keep the effort within a reasonable limit, the action of the airbag skirts was neglected. Nevertheless, it was decided that the g-levels shall be tested as they are defined. Therefore, all loads have to be taken by the airbag belts. Of course, this is a more stringent load case, where the structure is exposed to a high acceleration field. By neglecting the airbag skirt another drawback arises. Not all drop directions can be tested. Especially in lateral z-axis the SurfM would slip through the airbag belts (conf. Fig.11). For this reason the number of tests was reduced to the following two cases:

1. first bounce - upright
2. second bounce - upside-down

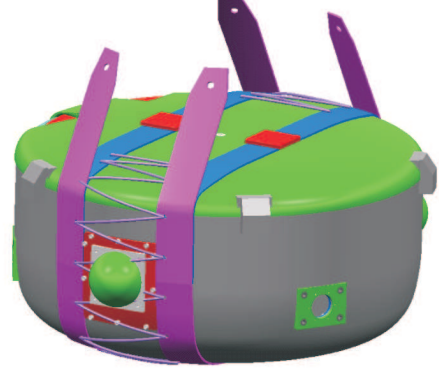


Figure 11. Airbag Belts Design

## 5.2. Preliminary Considerations

To evaluate the necessary drop height and spring stiffness in order to achieve the above mentioned drop shock profile knowing about the velocity change and the spring displacement is mandatory. The acceleration curve, velocity change and spring stiffness can be calculated as described by Steinberg (1999):

$$a(t) = A_0 \sin\left(\frac{\pi t}{T}\right) \quad (1)$$

$$\Delta v = \int_{t=0}^{t=t_1} a(t) dt = \frac{2A_0 t}{\pi} \cos\left(\frac{\pi t}{T}\right) \quad (2)$$

$$s = \int_{t=0}^{t=t_1} \Delta v dt \quad (3)$$

- $A_0$  ... acceleration amplitude
- $a$  ... acceleration
- $\Delta v$  ... velocity change
- $s$  ... chrash pad displacement
- $T$  ... half sine duration
- $t$  ... time

Furthermore, the drop height is calculated using the following formula with  $C = (1, 2)$  as a constant depending on the rebound properties:

$$\Delta v = C\sqrt{2gh} \quad h = \frac{\Delta v^2}{C^2 2g} \quad (4)$$

In order to generate a shock load of  $180g$  with a half sine profile and a  $20\text{ msec}$  duration, a drop height of  $h = 26\text{ m}$  would be necessary for zero rebound and  $h = 6.5\text{ m}$  for a full rebound. These values were not achievable under the given circumstances. By using a full rebound and reducing the half sine duration to  $10\text{ msec}$  the drop height can be reduced to  $h \approx 1.6\text{ m}$ . As so far, this load case was considered to be quasi-static wrt. the SurfM structure, this assumption will not be affected by the reduction of the shock duration. A half sine duration of  $20\text{ msec}$  is based on a frequency of  $25\text{ Hz}$ . By decreasing the duration to  $10\text{ msec}$  a frequency of  $50\text{ Hz}$  will be generated which is sufficiently lower than the first global eigenfrequency of the SurfM as they were determined in Section 4.

### 5.3. Test Setup Description

The tests were conducted at the premises of the DLR Institute of Composite Structures and Adaptive Systems in Braunschweig. A special test rig was designed allowing for a drop height of  $h \geq 1.7\text{ m}$ . In Fig. 12 there is shown the principle of the test device. The SurfM is positioned inside the airbag belts structure, which is fixed on a steel rod by means of an adapter. The test rig itself is a stiff steel construction. A crane will be used to lift the steel rod and the SurfM. For this reason a rope is fixed at the end of the steel rod. The other end of the rope is fastened on the test rig for easy access while cutting. After lifting the SurfM to the desired height the test will be conducted by cutting the rope.

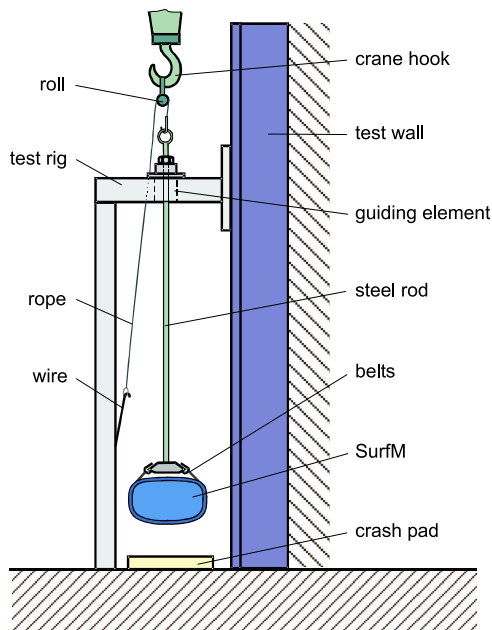


Figure 12. Drop In-Airbag Test Rig Principle

Since the airbag manufacturer could not provide original parts, the airbag belts were made based

on existing drawings using appropriate materials. In Fig. 13 there is shown the SurfM with mounted airbag belts.



Figure 13. Airbag Belts mounted on Surface Module

Throughout all tests one accelerometer was mounted either on top or bottom of the SurfM in order to check the generated g-load levels and profiles. The technical specifications of the data acquisition devices are described in the listings hereafter.

#### Data Acquisition:

acquisition system: LMS MIRAS  
software: LMS CADA-PC V.3.87.21

#### Acceleration Measurement: Accelerometers

company: PCB Piezotronics, Inc.  
type: 356 A 11  
frequency range:  $2\text{ Hz} - 10\text{ kHz}$   
acceleration range:  $\pm 500\text{ g}$   
max. shock:  $10000\text{ g}$   
resonant frequency:  $35\text{ kHz}$   
sensitivity voltage:  $10\text{ mV/g}$

### 5.4. Drop In-Airbag Test Results

Since the stiffness of the belts was not known, a great number of trials was necessary to approach the required specifications. After having performed a great variety of adjustment tests, it was finally possible to achieve the desired accelerations and half sine pulse durations using the described test rig. In Fig. 14 there is shown the test facility at DLR premises.

The acceleration-time histories, of the tests where the requirements were met, are shown in Fig. 15. Both were conducted using a drop height of  $h = 1.5\text{ m}$ . The resulting difference in the acceleration profile is traced back to the different stiffness properties of the airbag belts depending on the configuration to be tested.



Figure 14. In-Airbag-Drop Test Rig and Data Acquisition

As post-processing a 300 Hz low-pass filter was used to display the drop shock profile. This leads in upright position to a maximum acceleration of 189 g in a time duration of  $\approx 10$  msec. In case of the upside-down position the maximum acceleration is analyzed to be 125 g in a time duration of  $\approx 12$  msec.

All post test visual inspections did not reveal any damages, neither on the structure nor on any payload representative parts. As a result of the tests conducted, it can be stated, that the SurfM is capable of resisting the high g-level loads for bounces in upright and upside-down position. Based on this outcome the structural design was considered to be adequate at this stage of the project.

## 6. DROP OUT-OF-AIRBAG TESTING

### 6.1. General Remarks and Requirements

The drop out-of-airbag is also considered to be one of the most design driving load cases. It does not only affect the SurfM structure but also, due to its shock responses, is it very important for the payload design. A similar environment on the Beagle II Mars lander was the design driver for several of its payload units. Shock levels on the units on the impact on the ground were found to be over 300 g as outlined by Phillips (2000). Higher accelerations were recorded at pre-breadboard tests at DLR Braunschweig.

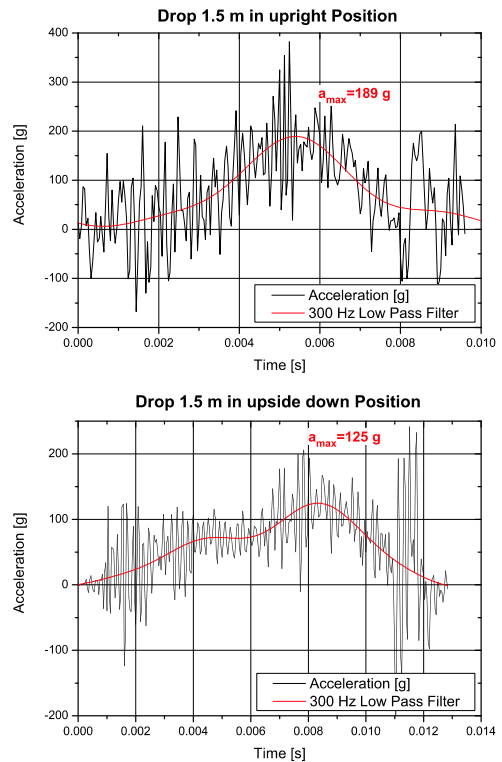


Figure 15. Drop In-Airbag Deceleration Profile

The SurfMSA shall withstand a free fall on the surface of Mars in any direction and from a maximum height of 1 m of its geometrical center.

The purpose of the tests is to:

- verify that the SurfM structure is not damaged to an extent that endangers the mission
- derive design acceleration levels for this load case for internal payloads

### 6.2. Test Set-up

The test set-up, as shown in Fig. 16, consists of the SurfM structure which will be lifted by a crane. Ropes will be used for a connection and also to position the SurfM for the different tests. Furthermore, there are the data acquisition devices and an appropriate ground simulant. Two ground properties were considered:

1. sand layer with approx. 5 cm thickness
2. aluminum plate with 5 cm thickness to simulate flat rock

To perform tests with the same physical characters like a drop on Mars the drop height has to be adjusted such that the model would have the same



Figure 16. Drop out-of-airbag Setup

impact velocity or energy. With Mars gravity of  $\approx 0.377g$  the impact velocity will be  $2.7\text{ m/s}$ . This leads to a drop height of  $0.4\text{ m}$  under Earth gravity. Taking into account that the drop height is defined wrt. the SurfM geometrical center the real drop height varies as the orientation of the SurfM changes as can easily be seen in Fig. 17. For drop along the y-axis the real drop height will be  $0.32\text{ m}$  and in lateral directions merely  $0.27\text{ m}$ . However the SurfM was tested from a drop height  $0.4\text{ m}$  in y-axis and  $0.3\text{ m}$  in lateral axes leading to some margin. All tests should be performed in  $\pm$  direction of each coordinate axis until reaching the maximum drop height.

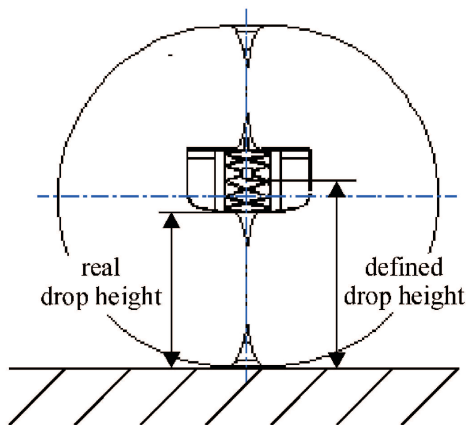


Figure 17. Drop Height Definition

Throughout all tests the acceleration time histories were recorded by using the same acquisition devices as for the drop in-airbag tests. Five tri-axial ac-

celerometers were mounted on different structural parts inside the SurfM structure. A sampling rate of  $25\text{ kHz}$  was chosen for data record allowing for good predictions to frequencies up to  $2500\text{ Hz}$  as it is stated by Irvine (2000).

### 6.3. Data Post Processing

After recording the acceleration-time histories, these data have to be further processed to enable the calculation of the SRS. In order to do this only two parts of the acceleration-time history have to be taken into account:

1. bounce onto sand or aluminum plate
2. free vibration after the shock until the amplitude of the vibration is sufficiently small

In Fig. 18 there are shown the different parts of the recorded response functions. These parts will be taken as input function to calculate the SRS, by applying these part of the acceleration-time history as base excitation to an array of SDOF (single degree of freedom) system. The natural frequency of the SDOF system is the independent variable. Therefore the calculation will be performed for a certain number of SDOF systems, each with a unique natural frequency. In this specific case a  $1/12$  octave bandwidth scheme was used. Each successive natural frequency will be  $2^{1/12}$  times the previous frequency. This is done for a frequency range of  $1\text{ Hz} \leq f_{nat} \leq 10000\text{ Hz}$ . The damping for each system was chosen to be  $Q = 10$ , which is similar to  $\zeta = 0.05$  critical damping.

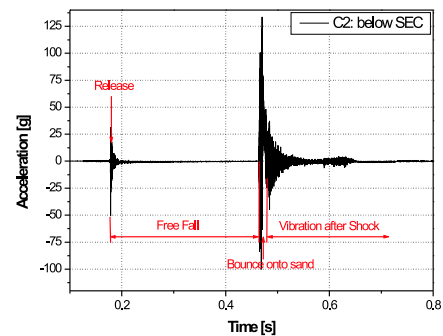


Figure 18. Windowing for SRS Analysis

### 6.4. Drop Out-of-Airbag Test Results

The SurfM structure was tested on sand and on an aluminum plate until reaching the maximum drop

heights. Fig. 19 shows a typical acceleration-time history for a test in y-direction on sand from maximum test in y-direction. Already during the inspection of the structural responses the drop on the aluminum plate turned out to be the heavier load case for structure and payloads.

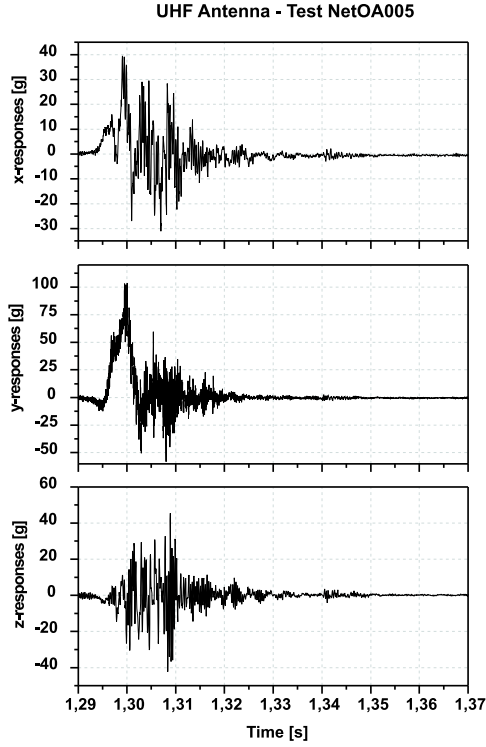


Figure 19. Typical Drop Acceleration-Time History

In Table 4 there are listed the tests performed at maximum drop height. This enables a better understanding of the final diagrams displayed in Fig. 20. Each single curve resembles the maximum structural responses in drop direction of all accelerometers for one test. It can clearly be seen that for each drop direction those curves form the upper boundary, which resemble the tests in this direction. Additionally, specifications are introduced in the diagrams. The shock levels enveloped by the derived specification do not exceed the specified shock levels induced by pyrotechnical events, as defined in the interface documentation.

Table 4. Maximum Height Drop Tests on Aluminium

Test No.	Direction	Height [m]
12	-Y	0.4
13	+Y	0.4
14	-X	0.3
15	+Z	0.3
16	-Z	0.3
17	-X	0.3

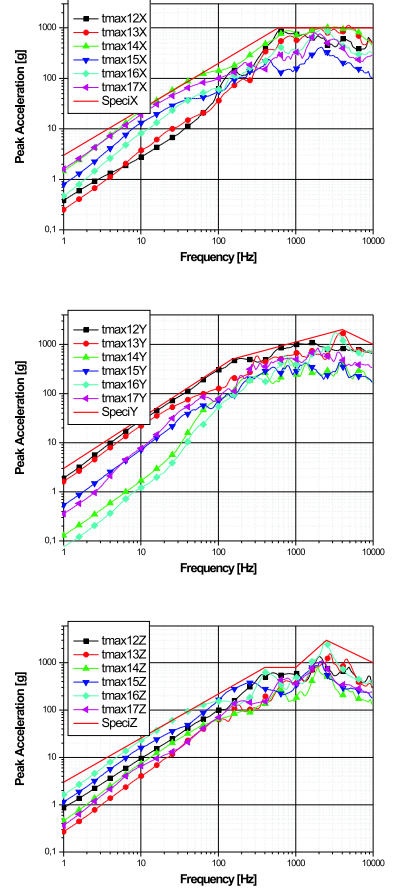


Figure 20. Shock Respose Spectra for Drop on Aluminium

Repeated testing of the breadboard model caused finally local structural damages, which could completely be avoided in the future by slight design improvements.

## 7. CONCLUSION AND FUTURE PROSPECT

Throughout the Mars Premier Project structure of the NetLander Surface Module was designed, built and tested at the DLR Institute of Composite Structures and Adaptive Systems until the end of Phase B.

In order to gain confidence in the structural design, tests were already conducted in such an early project phase. Particular interest was paid to the identification of the first eigenfrequencies and to the testing of the most stringent and design driving load cases, which are the first bounces on Martian ground inside the airbag and the drop out-of-airbag onto Martian ground.

In case of resonance search testing it could be ver-

ified, that the SurfM fulfills the stiffness criterion of  $f_{nat} \geq 150 \text{ Hz}$ . Furthermore, a good agreement between the tested and calculated eigenfrequencies could be noticed, whereas no attention was paid to the correlation of mode shapes.

In order to test the drop inside the airbag a test rig was constructed allowing to generate half sine deceleration profiles with maximum accelerations up to  $180g$  and a duration of  $\approx 10 \text{ msec}$ . These tests showed that the SurfM design is adequate to resist these loads.

Drop out-of-airbag tests were conducted for different soil conditions and until maximum drop heights, depending on the SurfM orientation. SRS were analyzed and specification issued.

By successful testing of this design driving load cases the SurfM design proved adequate for the mission scenario, up to this stage.

Throughout the NetLander project a cost effective lander structure was designed, built and tested. Although this project was stopped in the end of Phase B, the developed structure and the gained experiences can be a valuable heritage for future planetary, comet or asteroid missions.

## REFERENCES

- Ewins D.J., 1995, Modal Testing: Theory and Practice, Research Studies Press LTD., Taunton, England
- Cruise A.M., 1998, Bowles J.A., Patrick T.J. and Goodall C.V., Principles of Space Instrument Design, Cambridge University Press, Cambridge, United Kingdom
- Steinberg Dave S., 1999, Vibration Analysis for Electronic Equipment, John Wiley & Sons Inc., New York, USA
- Harris Cyril M., 1995, Shock and Vibration Handbook, McCraw-Hill, New York, USA
- Sarafin Thomas P., 1995, Spacecraft Structures and Mechanisms – From Concept to Launch, Microcosm Inc., Torrance, USA (CA)
- Irvine Tom, 2000, An Introduction to the Shock Response Spectrum,
- Irvine Tom, 2001, Integrating an Acceleration Half-Sine Pulse, [www.vibrationdata.com](http://www.vibrationdata.com)
- Irvine Tom, 2000, Simple Drop Shock, [www.vibrationdata.com](http://www.vibrationdata.com)
- Eriksson John and Hansson Mattias, 1999, Measuring and Analysis of Pyrotechnic Shock, Ph.D. Thesis, Chalmers University of Technology Göteborg
- Phillips Nigel, Mechanisms for the Beagle 2 Lander, Astrium Uk Ltd.